J. Fluid Mech. (1988), *vol.* 186, *pp.* 351–377
Printed in Great Britain

The effect of dead zones on longitudinal dispersion in streams

By ANTON PURNAMA

Department of Applied Mathematics and Theoretical Physics, University of Cambridge, Silver Street, Cambridge CB3 9EW, UK

(Received 6 August 1986 and in revised form 27 June 1987)

Dead zones tend to hold back the downstream travel, to increase the longitudinal spreading and to provide a long tail of low concentration for passive contaminant releases in natural streams. Here it is shown how the presence of a random distribution of dead zones can be accommodated into the method of moments by choosing an appropriate composite averaging. The individual roles of the cross-stream velocity shear, the dead-zones mean volume fraction and the dead-zones probability distribution are clearly revealed in the longitudinal shear-dispersion coefficient. The inevitable deviations from Gaussianity are examined by means of skewness and kurtosis. Simple examples are used to quantify the effects of the dead zones upon contaminant dispersion in Couette flow, pipe and plane Poiseuille flows.

1. Introduction

Dead zones are local areas of the flow cross-section with relatively still water or no net downstream velocity. These randomly isolated 'dead-water' regions are caused by the meandering nature of streams, debris and encroaching trees and vegetation along the sides of streams. The visual observation of non-buoyant tracers used for dispersion studies in natural streams indicates that a portion of tracer concentration is diffused into and is temporarily detained in the dead zones as the tracer cloud passes by, and is gradually released back into the main stream to move downstream again (Fischer 1967). A similar feature occurs in estuaries and other embayments (Okubo 1973). The dead zones are also found in the river bed where there are many roughness elements that provide small spaces for retaining part of the flow (Valentine & Wood 1977), and in an industrial pipe line in which stagnant fluid collects in the crevices of flanges, or at the hollows of a corroded surface. The most significant contribution of this temporary storage mechanism on the tracer concentration distribution is its production of a low-concentration tail. The resulting skewness is much greater than would result from the velocity shear effect alone (Nordin & Troutman 1980).

The complexity of the flow field and of mixing phenomena in natural streams force us to investigate an idealized case in which some of the general features of contaminant dispersion can be revealed analytically. Turner (1958) visualized a model of a flow system consisting of a main channel which has a uniform cross-sectional shape and area, through which the fluid flows. Communicating with the main channel are dead-end stagnant pockets of prismatic cross-section which are distributed uniformly along the length of the channel. There is no bulk flow into and out of these pockets and any exchange of contaminant between the main channel and stagnant pockets is by diffusion only. (For the purpose of the analysis the term

'pocket' is used to refer to the geometric feature of the dead zone.) Aris (1959), using a generalization of Turner's model which allows the stagnant pockets to have all possible depths opening on the circular channel, has shown how the presence of these pockets influences the longitudinal dispersion coefficient D, and noted that enhancement of D was related to the distribution of pocket depths, and not merely to the mean fraction void volume β. This result has been confirmed by the experimental work of Evans & Kenney (1966), who employed a retentive layer of stagnant gas held within a porous solid structure.

In the present paper, we generalize and extend Aris's results. By using an appropriate composite cross-sectional averaging, the effect of the probability distribution of stagnant-pocket depths can be incorporated into the conventional (no pockets) method of moments (Aris 1956). This eliminates the explicit occurrence of any pocket-depths probability distribution in the moment equations of the contaminant concentration distributions. Encouraged by this observation, we are able to calculate the first four moments in the presence of stagnant pockets, and to analyse the departures of contaminant concentration distributions from Gaussianity. Mean concentration distributions have then been calculated from the moments using Chatwin's (1970) Edgeworth series approximation.

2. Composite cross-sectional averaging

We shall consider a uniform, symmetric plane parallel flow of width $2a$; this is only for convenience and, in principle, the method can be extended to more general geometries (Aris 1956, §5). On the walls of this channel are the open mouths of stagnant pockets of various depths. It is assumed that the probability distribution of pocket depths does not vary along the channel length and that the longitudinal extent of an individual pocket is short compared with the channel diffusion lengthscale. The flow system then consists of the main flow with longitudinal velocity $u(y)$ and the stagnant pockets. There is no flow communicating between these two regions so diffusion is the only mechanism of transporting contaminant across their interface, i.e. the planes $y = 0, y = -2a$. By symmetry we can restrict our attention to one half of the flow (figure 1). Note that for the linear Couette flow (Appendix A) this is the full problem, i.e. the pocket only occupies one side of the flow (bottom).

Valentine & Wood (1977) pointed out that there are two variables that control the role of stagnant pockets on the dispersion process: the area proportion of the wall covered by pockets and the (individual) pocket depth. (In rivers these variables may be related in some complex manner.) To incorporate these two factors (Aris 1959) we assume that the stagnant-pocket depths al are distributed with a probability density function $p(l)$. By attributing to the wall area that is not a pocket mouth a pocket of depth zero, we have

$$p(l) = \alpha P(l) + (1-\alpha)\,\delta(l), \tag{2.1}$$

where α = constant is the probability (for each value of x) that there is a pocket of that value of x. In terms of $p(l)$, the mean ratio β of the total dead-water volume to that of the channel can be defined:

$$\beta = \{l\} = \int_0^\infty \mathrm{d}l\, lp(l) = \alpha \int_0^\infty \mathrm{d}l\, lP(l). \tag{2.2}$$

Here, the curly brackets denote ensemble averaging over the pocket-depths probability distribution.

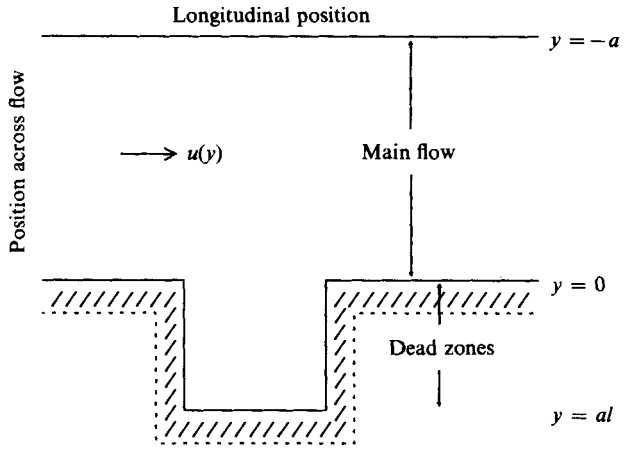

FIGURE 1. Schematic diagram of a channel with an idealized rectangular stagnant pocket.

A rusty pipe has an appreciable fraction of its void space 'dead' filled with stagnant fluid (Evans & Kenney 1966). For rivers Young & Wallis (1986) attribute all the dispersion to the dead zones, and they find from the skewness of the concentration distribution that values of β as large as 0.3 can be appropriate; whereas for a man-made (uniform concrete) channel with no dead zones this empirical value reduces to 0.15. It is the difference in β-values that can be truly attributed to the dead zones. Thus, we can estimate that $\beta = 0.15$ for natural streams.

Within any one pocket the concentration of a passive contaminant c_l depends crucially upon the depth al of that pocket. However, for the main flow the detailed $p(l)$ is unimportant (because the pockets are short) and can be averaged out. Thus, to distinguish concentrations in the two regions, we define

$$C = \begin{cases} c_l & \text{for} \quad 0 < y < al, \\ c & \text{for} \quad -a < y < 0. \end{cases} \tag{2.3}$$

A major difficulty in the work of Aris (1959) is in the occurrence of two modes of averaging: the ensemble averages over pocket-depths probability distribution and the cross-sectional averages (over the pocket depths and the main flow). The breakthrough which allowed the present work to extend that of Aris was the recognition that a composite averaging process, denoted here by a tilde, sufficed. For example, the composite cross-sectional area per unit channel depth A is defined as

$$A = \left\{ \int_{-a}^{al} \mathrm{d}y \right\} = a(1+\beta). \tag{2.4}$$

Hence the definition of composite cross-sectional average values includes ensemble averages over the pocket-depths probability distribution:

$$\tilde{C} = \frac{\left\{ \int_{-a}^{al} C \, \mathrm{d}y \right\}}{\left\{ \int_{-a}^{al} \mathrm{d}y \right\}} = \frac{\bar{c} + \{l\overline{c_l}\}}{1+\beta}. \tag{2.5}$$

Here the conventional cross-sectional averages over the main flow or over the pocket depths (separately) are given respectively by

$$\bar{c} = \frac{1}{a}\int_{-a}^{0} c\,\mathrm{d}y, \tag{2.6a}$$

$$\overline{c_l} = \frac{1}{al}\int_{0}^{al} c_l\,\mathrm{d}y. \tag{2.6b}$$

Note that when $\beta = 0$, i.e. no pockets, $\tilde{C} = \bar{c}$.

Furthermore, the composite cross-sectionally averaged value of the longitudinal velocity

$$U(y) = \begin{cases} 0 & \text{for} \quad 0 < y < al, \\ u(y) & \text{for} \quad -a < y < 0, \end{cases} \tag{2.7a}$$

is determined by

$$\tilde{U} = \frac{\bar{u}}{1+\beta}, \tag{2.7b}$$

which is the bulk velocity of contaminant cloud in the presence of stagnant pockets derived by Aris (1959), Okubo (1973) and Valentine & Wood (1977, equation (16*b*)). Note that it is smaller than the main-flow cross-sectional mean velocity $\bar{u}$. This reduction is due to the involvement of contaminant in the stagnant pockets: the larger the mean volume fraction the more time a contaminant spends there. The conservation of volume flow along the channel can be expressed as

$$A\tilde{U} = \text{constant}. \tag{2.8}$$

3. Concentration equations and the method of moments

In axes moving with the bulk velocity $\tilde{U}$, the equations that we seek to solve are:

in the stagnant pockets $(0 < y < al)$

$$\partial_t c_l - \tilde{U}\,\partial_x c_l - \partial_y(\kappa_l\,\partial_y c_l) = 0; \tag{3.1a}$$

in the main flow $(-a < y < 0)$

$$\partial_t c + (u-\tilde{U})\,\partial_x c - \partial_y(\kappa\,\partial_y c) = 0. \tag{3.1b}$$

In principle, the transverse diffusivity κ_l inside the pockets may differ from κ (Chatwin 1973), or from pocket to pocket. The effect of direct longitudinal diffusivity has been neglected. Evans & Kenney (1966) showed that, if required, this additional dispersive-mechanism term can simply be added to the shear-dispersion coefficient D.

Boundary conditions describing the continuity of transverse flux and the continuity of mass conservation at the interface $y = 0$ are

$$c = c_l, \tag{3.2a}$$

$$\kappa\,\partial_y c = \{\kappa_l\,\partial_y c_l\}. \tag{3.2b}$$

(We recall that for the main flow the pocket-depths probability distribution has been averaged out.) Zero-flux conditions are chosen on the main-flow axis of symmetry and on the pocket boundary so that

$$\kappa_l \partial_y c_l = 0 \quad \text{at } y = al, \tag{3.3a}$$

$$\kappa \partial_y c = 0 \quad \text{at } y = -a, \tag{3.3b}$$

and

$$\kappa \partial_y c = 0 \quad \text{on } \partial A, \tag{3.3c}$$

where ∂A is that part of the channel boundary which does not have any stagnant pockets.

The centroid, variance, skewness and kurtosis are direct properties of the first four moments of the contaminant concentration distributions. Thus, following Aris (1956), we introduce the moments both for the stagnant pockets and for the main flow:

$$c_l^{(n)} = \int_{-\infty}^{\infty} x^n c_l \, dx, \tag{3.4a}$$

$$c^{(n)} = \int_{-\infty}^{\infty} x^n c \, dx, \tag{3.4b}$$

with the composite cross-sectionally averaged moments

$$M^{(n)} = \int_{-\infty}^{\infty} x^n \tilde{C} \, dx, \tag{3.5}$$

and accordingly, we set

$$r_l^{(n)} = \int_{-\infty}^{\infty} x^n (c_l - \tilde{C}) \, dx, \tag{3.6a}$$

$$r^{(n)} = \int_{-\infty}^{\infty} x^n (c - \tilde{C}) \, dx \quad (n = 0, 1, 2, \ldots). \tag{3.6b}$$

As before capital letters C, R denote the concentration in both regions and lower-case letters the separate contributions. We shall also frequently use $U(y)$; however from (2.7a) this has only the main-flow velocity component $u(y)$ since the flow within any individual pocket is stagnant.

Taking moments of the advection–diffusion equations (3.1a, b), using the boundary conditions (3.2a, b) and (3.3a, b) (Smith 1985), we find that the successive composite zero-average terms $r_l^{(n)}$, $r^{(n)}$ satisfy the hierarchy equations

$$\partial_t r_l^{(n)} - \partial_y(\kappa_l \partial_y r_l^{(n)}) = -n\tilde{U} M^{(n-1)} - n(\tilde{U} r_l^{(n-1)} + \overbrace{(U - \tilde{U}) R^{(n-1)}}), \tag{3.7a}$$

with

$$\kappa_l \partial_y r_l^{(n)} = 0, \quad y = al, \tag{3.7b}$$

$$\left.\begin{aligned} r_l^{(n)} &= r^{(n)}, \\ \kappa \partial_y r^{(n)} &= \{\kappa_l \partial_y r_l^{(n)}\}, \end{aligned}\right\} \quad \text{at } y = 0, \tag{3.7c, d}$$

$$\partial_t r^{(n)} - \partial_y(\kappa \partial_y r^{(n)}) = n(u - \tilde{U}) M^{(n-1)} + n((u - \tilde{U}) r^{(n-1)} - \overbrace{(U - \tilde{U}) R^{(n-1)}}), \tag{3.7e}$$

with

$$\kappa \partial_y r^{(n)} = 0, \quad y = -a, \tag{3.7f}$$

where the tilde indicates the composite cross-sectional averaging defined in (2.5).

Since the intention of this paper is to incorporate the storage mechanism we shall, for simplicity, restrict our attention to the special case of a uniform (over the cross-

section) initial discharge: at $t = 0$ a unit amount of contaminant is located at the plane $x = 0$ (and the equilibrium is attained for the overall trapping and releasing rate of contaminant across the interface between the moving and stagnant fluids). Hence, at $t = 0$,

$$r_l^{(0)} = r_l^{(1)} = r_l^{(2)} = \ldots = 0, \tag{3.8a}$$

$$r^{(0)} = r^{(1)} = r^{(2)} = \ldots = 0. \tag{3.8b}$$

An important sequel in the method of moments is that the successive composite cross-sectionally averaged term $M^{(n)}(t)$ evolves in accordance with

$$d_t M^{(n)} = n\widetilde{(U-\tilde{U})\,R^{(n-1)}}. \tag{3.9}$$

For the particularly simple initial discharge conditions assumed in (3.8a, b) at $t = 0$, we have

$$M^{(0)} = 1 \quad \text{for } t > 0, \tag{3.10a}$$

$$M^{(n)} = n\int_0^t \mathrm{d}t' \widetilde{(U-\tilde{U})\,R^{(n-1)}} \quad (n = 1, 2, 3, \ldots). \tag{3.10b}$$

It deserves comment that formally (3.7a–f), (3.9) and (3.10a, b) are identical with the corresponding result of the conventional method of moments for the case with no pockets (Smith 1985, equations (2.4a–c) and (2.3a, b)) by having a tilde in place of an overbar. Indeed, what has been achieved through the introduction of the composite cross-sectional averaging is the elimination of any explicit occurrence of $p(l)$. Thus, in principle, we can straightforwardly adapt any results of the conventional (no-pockets) method of moments. More importantly, we can utilize these results to separate the effects of stagnant pockets from those of velocity-shear gradients.

Even with the restriction to uniform discharges it is a formidable task to solve (3.8a–f) for more than the first few moments (Barton 1983). Fortunately, this appears to be all that is necessary and, for many practical purposes, only the asymptotic large-time solutions are needed. Chatwin (1970) showed that at large times after discharge, in the absence of stagnant pockets, the variance and the skewness can be expressed in terms of a single shape function $g(y)$. Here, following Chatwin, we derive the asymptotic forms for variance, skewness (and kurtosis) using the modified shape function $G^{(1)}(y)$.

4. Centroid displacement function

The use of the composite cross-sectional averaging ensures that the pattern of calculation proceeds as in the much more familiar method of moments (Smith 1981b, 1985). For the conventional (no-pockets) situation the zeroth-moment solution for a uniform initial discharge is trivial:

$$R^{(0)} = r^{(0)} = 0. \tag{4.1}$$

The direct analogy to the with-pockets situation permits us to deduce that

$$R^{(0)} = \begin{cases} r_l^{(0)} = 0 & \text{for } 0 < y < al, \\ r^{(0)} = 0 & \text{for } -a < y < 0. \end{cases} \tag{4.2}$$

Hence, we infer that $C^{(0)}$ remains uniform across the flow and has the constant value $M^{(0)} = 1$ (3.10a). In other words, the amount of contaminant in the main flow remains $(1+\beta)^{-1}$ of the initial quantity released (Okubo 1973). This is also in agreement with the result of Valentine & Wood (1977, equation (15)) that the

amount of contaminant in each region is proportional to the respective region volumes.

The next ingredient in the method of moments is the centroid position of the contaminant cloud. For the conventional case of no pockets the asymptotic solution of (3.7*a–f*) with $n = 1$ has the form

$$R^{(1)} = r^{(1)} = g(y), \tag{4.3}$$

where the conventional centroid displacement function $g(y)$ satisfies the transverse diffusion equation (Chatwin 1970, equation (1.10); Smith 1982, equation (3.9))

$$\partial_y(\kappa\,\partial_y g) = \bar{u} - u, \quad \text{with } \kappa\,\partial_y g = 0 \quad \text{on } \partial A, \tag{4.4a}$$

and

$$\bar{g} = 0. \tag{4.4b}$$

Physically, $g(y)$ describes the dependence of the contaminant centroid in any filament on its position across the flow (Aris 1956). Alternatively, $g(y)$ is the shape factor for longest persisting concentration variants across the flow (Taylor 1953).

The analogy with the stagnant-pockets situation (a tilde replacing an overbar) permits us to infer, for large t, that

$$R^{(1)} = \begin{cases} g_l^{(1)} & \text{for } 0 < y < al, \\ g^{(1)} & \text{for } -a < y < 0. \end{cases} \tag{4.5}$$

The modified centroid displacement functions $g_l^{(1)}(y)$, $g^{(1)}(y)$ then satisfy the transverse diffusion equations

$$\partial_y(\kappa_l\,\partial_y g_l^{(1)}) = \tilde{U}, \quad \text{with } \kappa_l\,\partial_y g_l^{(1)} = 0, \quad y = al, \tag{4.6a}$$

$$\left.\begin{aligned} g_l^{(1)} &= g^{(1)}, \\ \kappa\,\partial_y g^{(1)} &= \{\kappa_l\,\partial_y g_l^{(1)}\}, \end{aligned}\right\} \quad \text{at } y = 0, \tag{4.6b,c}$$

$$\partial_y(\kappa\,\partial_y g^{(1)}) = \tilde{U} - u, \quad \text{with } \kappa\,\partial_y g^{(1)} = 0, \quad y = -a, \tag{4.6d}$$

and

$$\widetilde{G^{(1)}} = 0. \tag{4.6e}$$

In order to assess the role of stagnant pockets, by observing the forcing terms of (4.6*d*), we now make an important decomposition of $G^{(1)}(y)$, for constant κ_l, into parts associated with the main-flow velocity $u(y)$, the mean volume fraction β, and the stagnant-pocket properties:

$$(1+\beta)\,G^{(1)}(y) = \begin{cases} g(0) + \beta f(0) + E + \dfrac{\bar{u}}{\kappa_l}(\tfrac{1}{2}y^2 - aly), & 0 < y < al, \\ g + \beta f + E, & -a < y < 0. \end{cases} \tag{4.7a,b}$$

The conventional centroid displacement function (the main-flow associated term) $g(y)$ is defined by (4.4*a*, *b*). The term associated with the mean volume fraction $f(y)$ satisfies the equation

$$\partial_y(\kappa\,\partial_y f) = -u, \quad \text{with } \kappa\,\partial_y f = -\bar{u}a, \quad y = 0, \tag{4.8a}$$

$$\kappa\,\partial_y f = 0, \quad y = -a, \tag{4.8b}$$

and

$$\bar{f} = -g(0) - \beta f(0). \tag{4.8c}$$

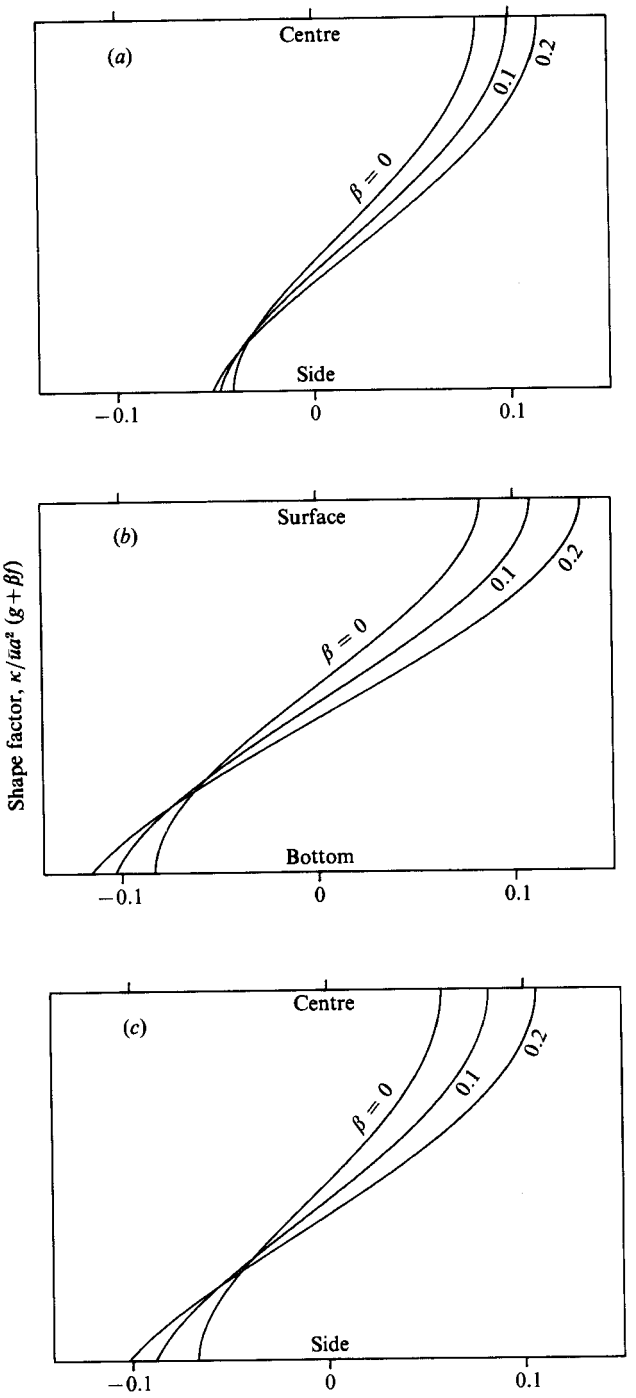

FIGURE 2. The shape factor $(\kappa/\bar{u}a^2)(g+\beta f)$ profiles across the flow. (*a*) Pipe Poiseuille flow; (*b*) Couette flow; (*c*) plane Poiseuille flow.

The effect of $p(l)$ on the centroid position of the contaminant cloud in the main flow is given by the stagnant-pocket property term

$$E = \frac{\bar{u}a^2\{l^3\}}{3\kappa_l(1+\beta)}. \tag{4.9}$$

This is determined by the constraint $\widetilde{G^{(1)}(y)} = 0$ (the necessary solvability condition for (4.6*a–e*) to have a unique solution). Note that E is independent of the shape of the main-flow velocity profile $u(y)$ and is proportional to the higher-order statistic term $\{l^3\}$ of $p(l)$.

If we substitute the result (4.2) into (3.10*b*) with $n = 1$, then we find, for large t, that

$$M^{(1)} = 0. \tag{4.10}$$

Hence, in axes moving with the bulk velocity the composite cross-sectionally averaged centroid of the contaminant cloud remains at the origin. The first moment itself has the limiting form

$$\frac{C^{(1)}}{C^{(0)}} = \frac{R^{(1)}}{M^{(0)}} \approx G^{(1)}, \tag{4.11}$$

so that the centre of mass of the contaminant cloud is distributed according to the modified centroid displacement function $G^{(1)}(y)$. Alternatively, by analogy with the case of no pockets, it can also be referred to as the shape factor.

Figure 2(*a–c*) shows the contribution to the shape factor from the main flow $g+\beta f$ as the mean volume fraction β is increased for the three types of flow considered in Appendix A. The development of backwards displacements close to the channel boundary is due to the condition of continuity of transverse flux at the interface between moving and stagnant fluids.

Following the notion that $g(y)$ is the (primary) shift of the conventional main-flow centroid between streamlines for the case with no pockets (Aris 1956, equation (24); Chatwin 1970, equation (1.9)), there is a (secondary) shift $\beta f(y)$ associated with the mean volume fraction β. This can be attributed to the fact that relative to the new reference velocity $\tilde{U}$ the main flow is slightly faster than before. Thus, in the main flow there is a corresponding forwards shift in the centroid displacement.

5. Shear-dispersion coefficient

The distinctive feature of the present analysis is that we seek to calculate the effect of stagnant pockets on the shear dispersion. We recall that the dispersion process of the contaminant is now due to (i) the combined effect of transverse diffusion and longitudinal shear velocity in the main flow, (ii) the continuous diffusion exchange at the interface between the moving and the stationary parts of the flow, and (iii) the effect of molecular diffusion within the stagnant pockets.

Continuing to the second moment (i.e. $n = 2$), (3.10*b*) becomes

$$M^{(2)} = 2t\widetilde{(U-\tilde{U})G^{(1)}} + 2\int_0^t \mathrm{d}t'\widetilde{(U-\tilde{U})(R^{(1)}-G^{(1)})}, \tag{5.1}$$

where we have made use of the asymptotic formulae (4.5) for $R^{(1)}$. By analogy with the case of no pockets, the coefficient of $2t$ gives us a formula for the longitudinal shear-dispersion coefficient D (Aris 1956, equation (40)):

$$D = \widetilde{(U-\tilde{U})G^{(1)}}. \tag{5.2}$$

The important feature of this generalization of Taylor's (1953) classic result is in the use of a tilde instead of an overbar, i.e. conventional instead of composite cross-sectional averaging.

In the absence of pockets, the positivity of D has been shown by Smith (1981*b*, equation (5.6)). Here (including the stagnant pockets) it can also be shown to be positive. First, we note from (4.6*a–e*), that

$$\kappa_l \partial_y g_l^{(1)} = \int_{al}^{y} \mathrm{d}y' \tilde{U}, \tag{5.3a}$$

and

$$\kappa \partial_y g^{(1)} = \int_{-a}^{y} \mathrm{d}y' (\tilde{U} - u). \tag{5.3b}$$

Next, by multiplying (4.6*a*, *d*) by $g_l^{(1)}(y)$ and $g^{(1)}(y)$ respectively, and then integrating by parts across the flow, we have

$$\widetilde{(U-\tilde{U})G^{(1)}} = D(\beta) + \frac{1}{1+\beta}\left\{\frac{1}{a}\int_0^{al} \mathrm{d}y \frac{1}{\kappa_l}\left(\int_{al}^{y} \mathrm{d}y' \tilde{U}\right)^2\right\}. \tag{5.4a}$$

The term for the contribution from the main flow, $D(\beta)$, depends only upon the main-flow properties $u(y)$, κ, and the mean volume fraction β:

$$D(\beta) = \frac{1}{1+\beta}\frac{1}{a}\int_{-a}^{0} \mathrm{d}y \frac{1}{\kappa}\left(\int_{-a}^{y} \mathrm{d}y' (u-\tilde{U})\right)^2. \tag{5.4b}$$

Moreover, when $\beta = 0$ (there are no pockets), it reduces to Taylor's (1953) result (Smith 1981*b*, equation (5.6)).

The second term of (5.4*a*) involves the stagnant-pocket properties κ_l, β and $p(l)$. For constant κ_l, we can show that

$$\frac{1}{1+\beta}\left\{\frac{1}{a}\int_0^{al} \mathrm{d}y \frac{1}{\kappa_l}\left(\int_{al}^{y} \mathrm{d}y' \tilde{U}\right)^2\right\} = \frac{\tilde{U}^2 a^2 \{l^3\}}{3\kappa_l(1+\beta)} = \frac{\bar{u}E}{(1+\beta)^2}. \tag{5.4c}$$

This is independent of the main-flow velocity shear distribution $u(y)$ and agrees with the approximation given by Chatwin (1973, equation (3.8)) to evaluate the effect of a viscous sublayer of height l. Chatwin estimated that (5.4*c*) contributes up to 20% to D. It also reveals that the mean cube of the stagnant-pocket depths alone affects the overall dispersion (see Appendix B).

An alternative decomposition of $D(\beta)$, using (4.7*a*, *b*) and the constraint $\widetilde{G^{(1)}(y)} = 0$, is

$$D(\beta) = \frac{\overline{(u-\bar{u})g} + \beta\overline{uf}}{(1+\beta)^2}. \tag{5.5}$$

We see that $D(\beta)$ consists of two distinct parts, each reflecting a different aspect of the dispersion process. As for the conventional case of no pockets, the first term arises from the interaction between longitudinal advection by the main-flow velocity shear and transverse diffusion, whereas the second term, from (4.8*a–c*), is the consequence of the effect of changed boundary conditions, namely the corrective diffusive transverse flux of the contaminant across the interface of the stagnant pockets and the main flow.

Figure 3 shows the contribution from the main flow to the dispersion coefficient $D(\beta)$ for constant κ as an increasing function of β for three special cases of Couette flow, pipe and plane Poiseuille flows (see Appendix A). The second term of (5.5)

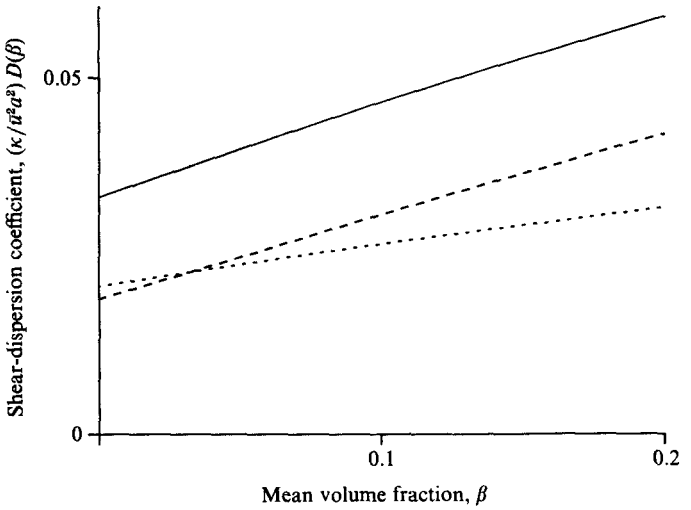

FIGURE 3. The dependence of the shear-dispersion coefficient $(\kappa/\bar{u}^2a^2)\,D(\beta)$ upon β for Couette flow (——), pipe Poiseuille flow (·····) and plane Poiseuille flow (– – –).

rapidly dominates the conventional (Taylor) shear-dispersion prediction. For $\beta = 0.2$, $D(\beta)$ is almost doubled.

Similarly, from (4.4*a*, *b*) and (4.8*a*–*c*), we can obtain an even more revealing formula for the total shear-dispersion coefficient D:

$$(1+\beta)^2 D = \frac{1}{a}\int_{-a}^{0} dy \frac{1}{\kappa}\left(\int_{-a}^{y} dy'(u-\bar{u})\right)^2 + \beta\frac{1}{a}\int_{-a}^{0} dy\left[\frac{1}{\kappa}\left(\int_{-a}^{y} dy' u\right)^2 - \frac{1}{1+\beta}\left(\int_{y}^{0} dy' \frac{\bar{u}}{\kappa}\int_{-a}^{y'} dy''\bar{u}\right)\right] + \frac{\bar{u}^2a^2\{l^3\}}{3\kappa_l(1+\beta)}. \quad (5.6)$$

This agrees with and extends the work of Aris (1959). The formula demonstrates the individual contributions of the main-flow velocity, the mean volume fraction β, and the higher-order statistics of $p(l)$ via $\{l^3\}$.

6. Variance

Here we are concerned with the composite cross-sectionally averaged second moment $M^{(2)}$ at large times after discharge. Although at first sight it might seem awkward to deal directly with the second term of (5.1), it happens, as shown by Smith (1981*b*), that the integrand is more tractable than the transient $R^{(1)}$. We avoid these intermediate mathematical details by using the procedure of the previous sections, that the method of moments with stagnant pockets can be treated as a generalization of the conventional (no-pockets) method of moments with a tilde in the place of an overbar.

For the no-pockets case, the final asymptotic formula for $M^{(2)}$ (Chatwin 1970, equation (3.8)) is

$$M^{(2)}_{\infty} = 2t\overline{(u-\bar{u})g} - 2\overline{g^2}. \quad (6.1)$$

Replacing the overbar by a tilde we infer, when there are stagnant pockets, that

$$M^{(2)}_{\infty} = 2t\widetilde{(U-\tilde{U})G^{(1)}} - 2\widetilde{(G^{(1)})^2}. \quad (6.2)$$

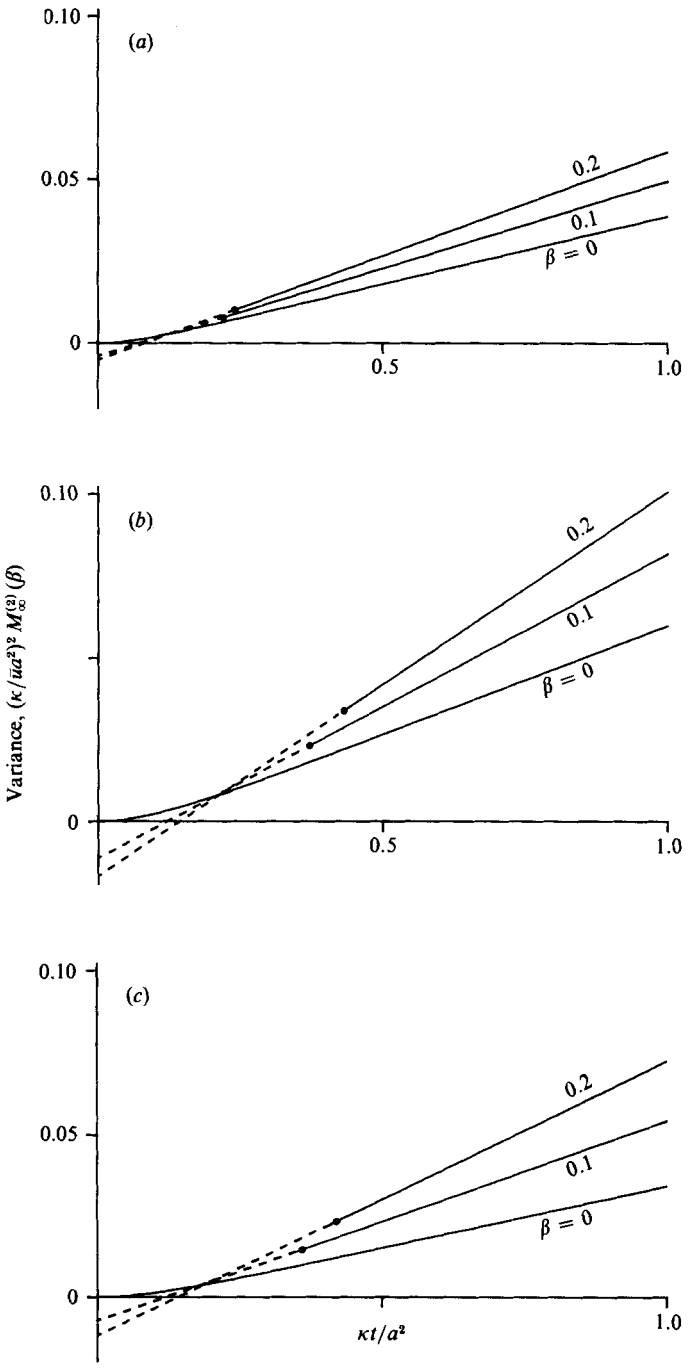

FIGURE 4. The variance $(\kappa/\bar{u}a^2)^2 M_\infty^{(2)}(\beta)$ as a function of $\kappa t/a^2$ with Barton's (1983) exact results for $\beta = 0$. ●, $3t_e(\beta)$ after which time the asymptotic result (6.4*b*) becomes pertinent. (*a*) Pipe Poiseuille flow; (*b*) Couette flow; (*c*) plane Poiseuille flow.

The first term represents the balance between the longitudinal stretching effect of the velocity shear and the transverse diffusion which, by acting together, increase $M_\infty^{(2)}$ steadily with time. In contrast, the second term is time-independent, embodying the overall effect of the early stages of dispersion on the variance, when large variations in the concentration exist across the flow rather than some equilibrium state.

The $-2\widetilde{(G^{(1)})^2}$ term makes the asymptotic variance (6.2) less than $2tD$. In the absence of stagnant pockets, this deficit variance was first pointed out by Chatwin (1970). Its negative contribution can be attributed to the initial inefficiency of the shear dispersion process, and in the Gaussian approximation (Smith 1982) its influence upon the concentration distributions only decays as $t^{-\frac{1}{2}}$. Next, using the decompositions (4.7*a*, *b*) for $G^{(1)}(y)$, we can decompose $\widetilde{(G^{(1)})^2}$ into terms associated with the main-flow property, the stagnant-pocket property and the pocket-depths-statistics cross-term:

$$\widetilde{(G^{(1)})^2} = \widetilde{(G^{(1)})^2}(\beta) + \frac{\bar{u}H}{(1+\beta)^2} + \frac{2E\bar{f}}{(1+\beta)^2}, \tag{6.3a}$$

the main-flow-related contribution term is given by

$$(1+\beta)^3\,\widetilde{(G^{(1)})^2}(\beta) = \overline{(g+\beta f)^2} + \beta\bar{f}^2, \tag{6.3b}$$

and the stagnant-pocket property term (independent of the shape of the main-flow velocity profile $u(y)$) is

$$\bar{u}H = \frac{\bar{u}^2a^4}{45\kappa_l^2(1+\beta)^2}[6(1+\beta)\{l^5\} - 5\{l^3\}^2]. \tag{6.3c}$$

The asymptotic composite cross-sectional averaged variance (6.2) becomes

$$M_\infty^{(2)} = M_\infty^{(2)}(\beta) + 2E\frac{\bar{u}t - 2\bar{f}}{(1+\beta)^2} - 2\frac{\bar{u}H}{(1+\beta)^2}, \tag{6.4a}$$

where the main-flow-related contribution to the variance is defined by

$$M_\infty^{(2)}(\beta) = 2t\frac{\overline{(u-\bar{u})g} + \beta\bar{u}f}{(1+\beta)^2} - 2\frac{\overline{(g+\beta f)^2} + \beta\bar{f}^2}{(1+\beta)^3}. \tag{6.4b}$$

In this definition the stagnant-pocket property terms E, H, and the higher-order pocket-depths statistics cross-term $E\bar{f}$ contributions have been excluded. (This is to emphasize the role of the mean volume fraction β without our needing to involve particular $p(l)$.)

Figure 4(*a–c*) shows the variance $M_\infty^{(2)}(\beta)$ as functions of β and t for the three type of flows considered in Appendix A. The two elements of (6.4*b*) can clearly be seen, the eventual linear growth but with a delayed effective starting time.

7. Decay rate

Although the above analysis does illuminate the effects of stagnant pockets upon contaminant dispersion, it does not provide a test for the accuracy of the asymptotic large-time approximation. To do this we introduce Taylor's (1953) concept of the time of decay to measure the longest persisting transverse variation of concentration, which is associated with the value of the decay rate, λ. Smith (1981*a*, equation (5.9)), for the case with no pockets, formulated the decay rate as

$$\lambda = \frac{\overline{(u-\bar{u})g}}{\bar{g}^2}. \tag{7.1}$$

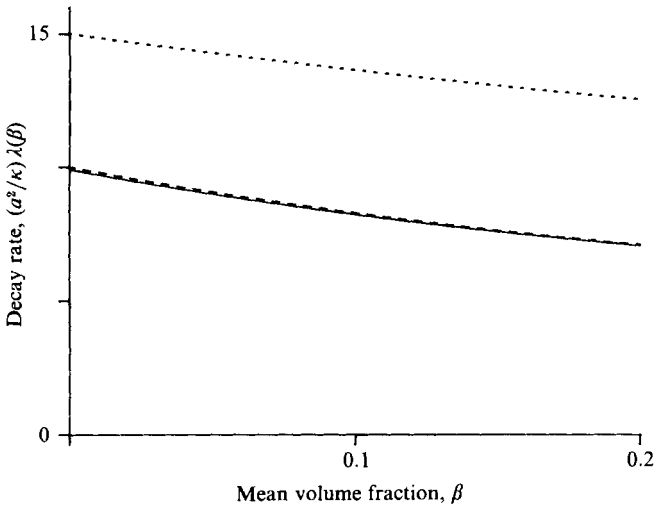

FIGURE 5. The decay rate $(a^2/\kappa)\lambda(\beta)$ for pipe Poiseuille flow (·····), plane Poiseuille flow (– – –) and Couette flow (——) as a function of β.

The obvious generalization is

$$\lambda = \frac{\widetilde{(U-\tilde{U})G^{(1)}}}{\widetilde{(G^{(1)})^2}}, \tag{7.2}$$

with the term for the contribution from the main flow

$$\lambda(\beta) = (1+\beta)\frac{\overline{(u-\bar{u})g} + \beta\overline{uf}}{\overline{(g+\beta f)^2} + \beta\bar{f}^2}. \tag{7.3}$$

The e-folding time related to the main flow, $t_e(\beta)$, for the free decay of the transverse concentration variations can be defined as

$$t_e(\beta) = \frac{1}{\lambda(\beta)}. \tag{7.4}$$

In the absence of stagnant pockets, the cross-sectional mixing can be regarded as having been established after about $3t_e$. It is the continual regeneration of concentration variations in regions of high concentration gradient which prolongs this influence of the earlier stages of dispersion.

Figure 5 shows the decay rate $\lambda(\beta)$ for constant κ as a function of β in pipe and plane Poiseuille flows and Couette flow (see Appendix A). As we might expect, $\lambda(\beta)$ is a monotonic decreasing function of β. Increasing the pocket depth al increases the distance over which the contaminant has to be diffused, thus requiring a greater time. It must be remembered that this also means greater β, which makes the effect on the bulk-contaminant cloud velocity $\tilde{U}$ less significant. Indeed, the decay rate is reduced by at least one-fifth when $\beta = 0.2$. Thus, the addition of stagnant pockets delays the occurrence of the 'Taylor regime' for which the rate of growth of the variance is linear with time (Valentine & Wood 1977).

8. Third moment

A linear growth of the variance with t is not sufficient to ensure that the distribution of contaminant concentration is Gaussian. Nordin & Troutman (1980) have emphasized the persistence of skewness in the observed concentration distributions. Hence, we shall pursue the analysis to calculate the deviations from Gaussianity as measured by skewness and kurtosis. Such deviations are not described by the longitudinal diffusion equation (Chatwin 1980).

In the conventional case with no pockets, Chatwin (1970, equation (3.9)) has shown, for large t, that the cross-sectional average third moment can be formulated as

$$M_\infty^{(3)} = 6t\overline{(u-\bar{u})g^2} - 12\overline{gg^{(2)}}. \tag{8.1}$$

By analogy with $g(y)$, the conventional variance function $g^{(2)}(y)$ satisfies the equation (Chatwin 1970, equation (2.12); Smith 1982, equation (3.11))

$$\partial_y(\kappa\,\partial_y g^{(2)}) = \overline{(u-\bar{u})g} - (u-\bar{u})g, \quad \text{with } \kappa\,\partial_y g^{(2)} = 0 \quad \text{on } \partial A, \tag{8.2a}$$

and

$$\overline{g^{(2)}} = 0. \tag{8.2b}$$

The necessary modifications of (8.1) for the introduction of stagnant pockets are

$$M_\infty^{(3)} = 6t\widetilde{(U-\tilde{U})(G^{(1)})^2} - 12\widetilde{G^{(1)}G^{(2)}}. \tag{8.3}$$

Here, by analogy with (4.6a–e) for $G^{(1)}(y)$, the modified variance function $G^{(2)}(y)$ satisfies the equations

$$\partial_y(\kappa_l\,\partial_y g_l^{(2)}) = \tilde{U}g_l^{(1)} + (U-\tilde{U})G^{(1)}, \tag{8.4a}$$

with

$$\kappa_l\,\partial_y g_l^{(2)} = 0, \quad y = al, \tag{8.4b}$$

$$\left.\begin{aligned} g_l^{(2)} &= g^{(2)}, \\ \kappa\,\partial_y g^{(2)} &= \{\kappa_l\,\partial_y g_l^{(2)}\}, \end{aligned}\right\} \quad \text{at } y = 0, \tag{8.4c,d}$$

$$\partial_y(\kappa\,\partial_y g^{(2)}) = (\tilde{U}-u)g^{(1)} + (U-\tilde{U})G^{(1)}, \tag{8.4e}$$

with

$$\kappa\,\partial_y g^{(2)} = 0, \quad y = -a, \tag{8.4f}$$

and

$$\widetilde{G^{(2)}} = 0. \tag{8.4g}$$

In order to evaluate the effect of the stagnant pockets, using decompositions (4.7a, b) for $G^{(1)}(y)$, we separate $\widetilde{(U-\tilde{U})(G^{(1)})^2}$ into terms associated with the main-flow and the stagnant-pockets properties, and the pocket-depths statistics cross-term:

$$\widetilde{(U-\tilde{U})(G^{(1)})^2} = \widetilde{(U-\tilde{U})(G^{(1)})^2}(\beta) + \frac{\bar{u}L}{(1+\beta)^3} + 2E\left(\frac{D(\beta)}{1+\beta} - \frac{\bar{u}\bar{f}}{(1+\beta)^3}\right), \tag{8.5a}$$

where the term for the contribution from the main flow is given by

$$(1+\beta)^4\,\widetilde{(U-\tilde{U})(G^{(1)})^2}(\beta) = \overline{(u-\bar{u})(g+\beta f)^2} + \beta(\overline{u(g+\beta f)^2} - \bar{u}\bar{f}^2), \tag{8.5b}$$

and the stagnant-pocket property term (independent of the distribution of main-flow velocity $u(y)$) is

$$L = \frac{2\bar{u}^2a^4}{45\kappa_l^2(1+\beta)^2}[-3(1+\beta)\{l^5\} + 5\{l^3\}^2]. \tag{8.5c}$$

As pointed out in §6, this separation into β-, L- and E-terms is to emphasize the role of the mean volume fraction β, without our needing to involve any particular $p(l)$.

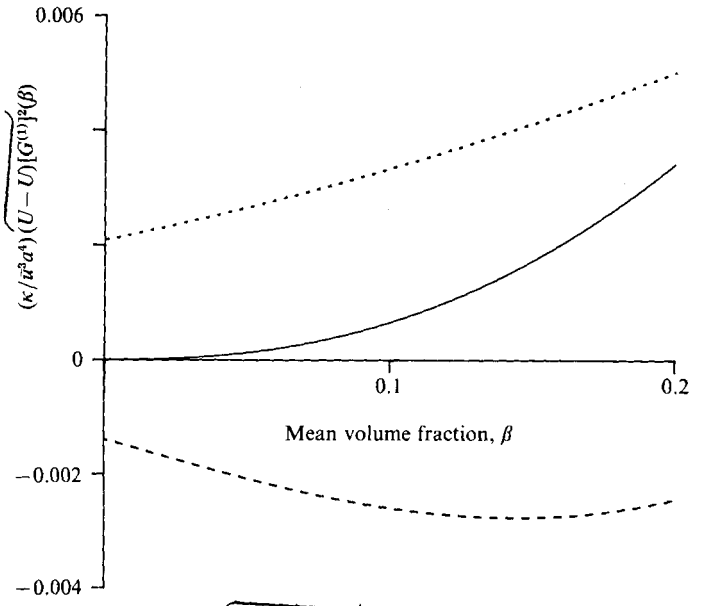

FIGURE 6. The values of $(\kappa^2/\bar{u}^3a^4)\overline{(U-\tilde{U})(G^{(1)})^2}(\beta)$ as a function of β for pipe Poiseuille flow (·····), Couette flow (——) and plane Poiseuille flow (– – –).

Figure 6 shows the dependence of $\overline{(U-\tilde{U})(G^{(1)})^2}(\beta)$ for constant κ, upon the mean volume fraction β for pipe Poiseuille flow, Couette flow and plane Poiseuille flow (see Appendix A). The domination of the main-flow velocity profiles is clearly exhibited for small β. However, this effect is rapidly suppressed with increasing β, and the general trend of increasing values of (8.5*b*) is evident with $\beta = 0.2$.

Since the algebra becomes unwieldly, it is desirable to eliminate the occurrence of $G^{(2)}(y)$ in favour of some more readily calculated function. In the absence of pockets, Chatwin (1970, appendix B) showed that

$$\overline{gg^{(2)}} = \overline{(u-\bar{u})Ig}, \tag{8.6}$$

where the additional auxiliary function $I(y)$ satisfies the equation (Smith 1982, equation (3.11))

$$\partial_y(\kappa\partial_y I) = -g, \quad \text{with } \kappa\partial_y I = 0 \quad \text{on } \partial A, \tag{8.7a}$$

and

$$\bar{I} = 0. \tag{8.7b}$$

Again, by the introduction of stagnant pockets, we have the equivalent form of (8.6) as

$$\overline{G^{(1)}G^{(2)}} = \overline{(U-\tilde{U})\mathscr{I}^{(1)}G^{(1)}}, \tag{8.8}$$

where the modified auxiliary function $\mathscr{I}^{(1)}$ satisfies the equations

$$\partial_y(\kappa_l\partial_y I_l^{(1)}) = -g_l^{(1)} \quad \text{with } \kappa_l\partial_y I_l^{(1)} = 0, \quad y = -al, \tag{8.9a}$$

$$\left.\begin{aligned} I_l^{(1)} &= I^{(1)}, \\ \kappa\partial_y I^{(1)} &= \{\kappa_l\partial_y I_l^{(1)}\}, \end{aligned}\right\} \quad \text{at } y = 0, \tag{8.9b, c}$$

$$\partial_y(\kappa\partial_y I^{(1)}) = -g^{(1)}, \quad \text{with } \kappa\partial_y I^{(1)} = 0, \quad y = -a, \tag{8.9d}$$

and

$$\overline{\mathscr{I}^{(1)}} = 0. \tag{8.9e}$$

Note that, from (4.6*a–e*) and (8.9*a–e*), it is straightforward to derive the identity

$$\widetilde{(U-\tilde{U})\mathscr{I}^{(1)}} = \widetilde{(G^{(1)})^2}. \tag{8.10}$$

Next, in order to analyse the effect of $p(l)$, by analogy with (4.7*a*, *b*) for $G^{(1)}(y)$, and for constant κ_l, we are led to decompose $\mathscr{I}^{(1)}(y)$ as

$$(1+\beta)\mathscr{I}^{(1)} = \begin{cases} I(0)+\beta J_{(1)}(0)+EJ_{(2)}(0)+H-\dfrac{E-\bar{f}}{\kappa_l}(\frac{1}{2}y^2-aly) \\ \quad -\dfrac{\bar{u}}{\kappa_l^2}(\frac{1}{24}y^4-\frac{1}{6}aly^3+\frac{1}{3}(al)^3y), \quad 0<y<al, & (8.11a) \\ I+\beta J_{(1)}+EJ_{(2)}+H, \quad -a<y<0. & (8.11b) \end{cases}$$

The conventional auxiliary function (the term associated with the main flow) $I(y)$ is defined in (8.7*a*, *b*). The term associated with the main volume fraction $J_{(1)}(y)$ satisfies the equation

$$\partial_y(\kappa\partial_y J_{(1)}) = -f, \quad \text{with } \kappa\partial_y J_{(1)} = -a\bar{f}, \quad y=0, \tag{8.12a}$$

$$\kappa\partial_y J_{(1)} = 0, \quad y=-a, \tag{8.12b}$$

and

$$\overline{J_{(1)}} = -I(0)-\beta J_{(1)}(0). \tag{8.12c}$$

The term associated with the stagnant-pocket-depth statistic $J_{(2)}(y)$ satisfies

$$\partial_y(\kappa\partial_y J_{(2)}) = -1, \quad \text{with } \kappa\partial_y J_{(2)} = -a, \quad y=0, \tag{8.13a}$$

$$\kappa\partial_y J_{(2)} = 0, \quad y=-a, \tag{8.13b}$$

and

$$\bar{u}\overline{J_{(2)}} = (1+\beta)\bar{f}-\beta\bar{u}J_{(2)}(0). \tag{8.13c}$$

The effect of $p(l)$ is represented by the stagnant-pocket-property term H (6.3*c*). However, this can also be determined by the constraint

$$\widetilde{\mathscr{I}^{(1)}(y)} = 0.$$

As in the case for E (4.9), H is independent of the shape of main-flow velocity profile $u(y)$ and is proportional to the higher-order statistic terms $\{l^5\}$ and $\{l^3\}$ of $p(l)$.

Using the decompositions (4.7*a*, *b*) and (8.11*a*, *b*), and from (8.8), the main-flow-related contribution to $\widetilde{G^{(1)}G^{(2)}}$ is given by

$$(1+\beta)^4\widetilde{G^{(1)}G^{(2)}}(\beta) = \overline{(u-\bar{u})(g+\beta f)(I+\beta J_{(1)})}+\beta[\overline{u(g+\beta f)(I+\beta J_{(1)})}-\bar{u}\bar{f}\,\overline{J_{(1)}}]. \tag{8.14}$$

Hence, we can denote the main-flow-related contribution to the composite cross-sectionally averaged third moment, for large t, by analogy with (6.4*b*) for $M_\infty^{(2)}(\beta)$, as

$$\begin{aligned}(1+\beta)^4 M_\infty^{(3)}(\beta) = {} & 6t(\overline{(u-\bar{u})(g+\beta f)^2}+\beta[\overline{u(g+\beta f)^2}-\bar{u}\bar{f}^2]) \\ & -12(\overline{(u-\bar{u})(g+\beta f)(I+\beta J_{(1)})}+\beta[\overline{u(g+\beta f)(I+\beta J_{(1)})}-\bar{u}f\,\overline{J_{(1)}}]). \end{aligned} \tag{8.15}$$

Figure 7 (*a–c*) shows the third moment $M_\infty^{(3)}(\beta)$ with increasing β for the three types of flow considered in Appendix A. The gradual release of the trapped contaminant helps to increase the contribution from the main flow to the skewness (see §9).

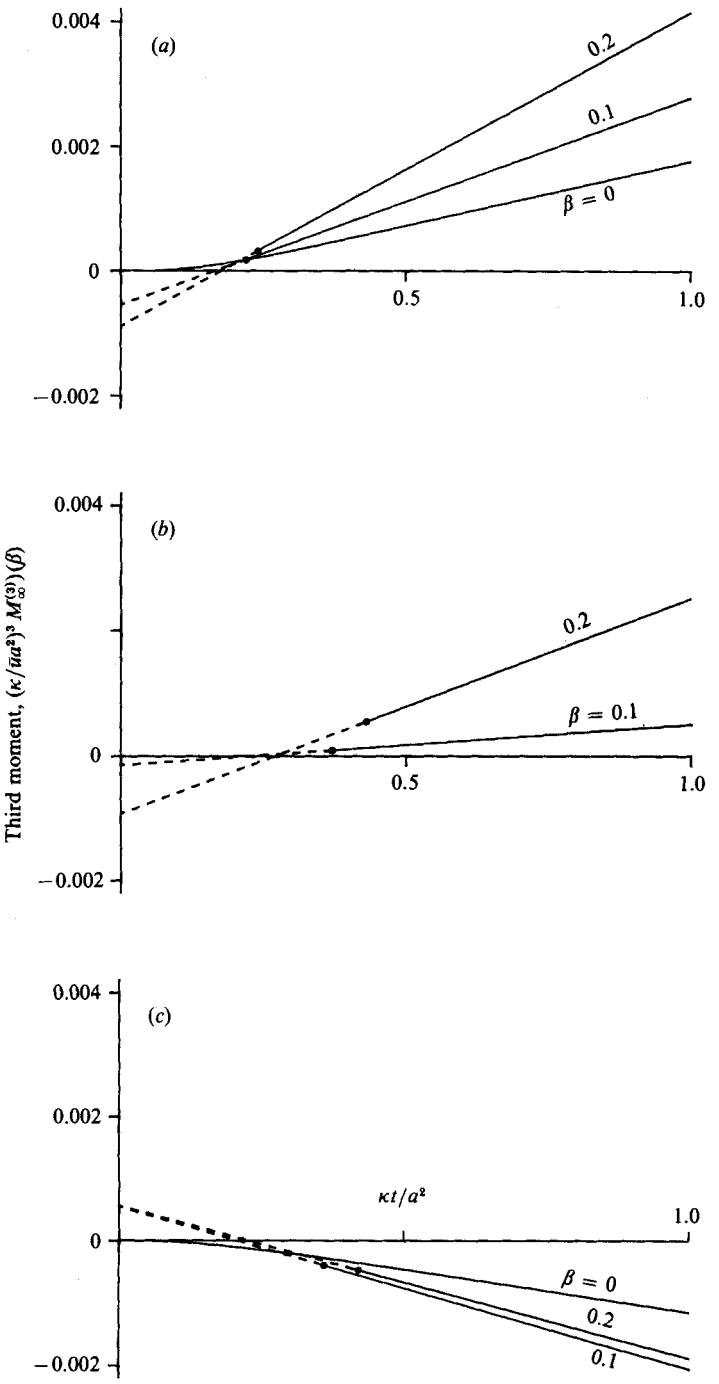

FIGURE 7. The third moment $(\kappa/\bar{u}a^2)^3 M_\infty^{(3)}(\beta)$ as a function of $\kappa t/a^2$ with Barton's (1983) exact results for $\beta = 0$. ●, $3t_e(\beta)$ after which time the asymptotic result (8.15) becomes pertinent. (*a*) Pipe Poiseuille flow; (*b*) Couette flow; (*c*) plane Poiseuille flow.

9. Skewness

The skewness S indicates the departure of a curve from symmetry. It is defined by the relationship

$$S = \frac{M^{(3)}}{(M^{(2)})^{\frac{3}{2}}}, \tag{9.1}$$

and by combining together the asymptotic results (8.3) for $M_\infty^{(3)}$ and (6.2) for $M_\infty^{(2)}$, we can infer that the skewness S has the asymptote

$$S \sim \frac{6t\overline{(U-\tilde{U})(G^{(1)})^2}}{[2t\overline{(U-\tilde{U})}\,G^{(1)}]^{\frac{3}{2}}}, \tag{9.2}$$

which decays at the slow rate $t^{-\frac{1}{2}}$ (Aris 1956; Chatwin 1970). Note that all quantities are given explicitly in terms of the modified shape function $G^{(1)}(y)$, and the velocity profile $U(y)$. The equivalent formula for the case without stagnant pockets is given by Smith (1981*b*, appendix A). Moreover, as was noted by Smith, it is independent of any initial contaminant distribution.

Using the results (8.5*a–c*) and (5.4*a–c*), we can separate the higher-order terms for the pocket-depths statistic from (9.2), and redefine the contribution to skewness from the main flow as

$$S(\beta) = \frac{6t(\overline{(u-\bar{u})(g+\beta f)^2}+\beta[\overline{u(g+\beta f)^2}-\bar{u}\overline{f^2}])}{(1+\beta)(2t[\overline{(u-\bar{u})g}+\beta\overline{uf}])^{\frac{3}{2}}}. \tag{9.3}$$

In the absence of stagnant pockets, the skewness can be positive (Aris 1956, equation (27)), identically zero (Barton 1983, equation (4.2*b*)), or even negative (Jayaraj & Subramanian 1978, fig. 13). As pointed out by Smith (1981*a*), the tendency to develop positive or negative skewness can be related to whether a smaller fraction of the flow is fast or slow moving as the tails of the contaminant distribution are associated with these regions. The presence of stagnant pockets enhances the faster-moving central region (figure 2*a–c*), hence the convective skewness is gradually overshadowed by the trapped contaminant in the tail of the concentration distribution. The second term in the numerator of (9.3) dominates (see figure 6), and for large β, $S(\beta)$ increases as $\beta^{\frac{1}{2}}$.

The positive skewness means a rapid surge of concentration when the contaminant arrives at the monitoring position, followed by a more gradual decay. Hence, the concentration peak will be displaced to the left of the centroid displacement (Okubo 1973, §3). As the contaminant moves downstream, transverse corrective fluxes are generated which remove contaminant to the pockets at the front and unload contaminant into the main flow at the rear.

10. Fourth moment and the kurtosis

After some algebra and omitting lengthy details, the composite cross-sectionally averaged fourth moment $M^{(4)}$ is finally found, for large t, to be

$$M_\infty^{(4)} - 3(M_\infty^{(2)})^2 = 24tK^{(4)} + 12[\overline{(G^{(1)})^2}]^2 - 24\overline{(G^{(2)})^2} + 24\overline{(U-\tilde{U})G^{(1)}}\,\overline{G^{(1)}\mathscr{F}^{(1)}} - 48\overline{(U-\tilde{U})\mathscr{F}^{(1)}G^{(2)}}, \tag{10.1a}$$

where

$$K^{(4)} = \overline{(U-\tilde{U})G^{(1)}G^{(2)}} - \overline{(G^{(1)})^2}\,\overline{(U-\tilde{U})G^{(1)}}. \tag{10.1b}$$

As pointed out by Chatwin (1970, this eventually grows linearly with time. Again, the time-dependent part of (10.1a) does not depend upon the initial discharge non-uniformity.

Chatwin (1980) proposed an alternative means of classifying longitudinal dispersion, which demanded that not only the skewness but also the kurtosis ought to be calculated or inferred from the observed concentration profiles. For if the concentration distribution were exactly Gaussian, both skewness and kurtosis would be identically zero. Thus, any approach to Gaussianity can be assessed by determining how these quantities decrease as functions of measuring position (or time).

The kurtosis (spikiness) K is defined by

$$K = \frac{M^{(4)} - 3(M^{(2)})^2}{(M^{(2)})^2}, \tag{10.2a}$$

hence it has the asymptote

$$K = \frac{24tK^{(4)}}{[2t\overline{(U-\tilde{U})G^{(1)}}]^2} \tag{10.2b}$$

which decays at the rate t^{-1}. Thus, at large time, K is less important than S.

The usefulness of (10.2b) depends upon the ease with which we can manipulate the modified shape function $G^{(1)}(y)$. It deserves emphasis that all quantities in (10.2b) can be given explicitly in terms of integrals involving $G^{(1)}(y)$, the diffusivities κ_l and κ, and the velocity profile $U(y)$. From (8.4a–g), we can derive

$$(1+\beta)\overline{(U-\tilde{U})G^{(1)}G^{(2)}} = \frac{1}{a}\int_{-a}^{0} \mathrm{d}y \frac{1}{\kappa}\left(\int_{-a}^{y} \mathrm{d}y'[(\tilde{U}-u)g^{(1)} + \overline{(U-\tilde{U})G^{(1)}}]\right)^2$$
$$+\left\{\frac{1}{a}\int_{0}^{al} \mathrm{d}y \frac{1}{\kappa_l}\left(\int_{y}^{al} \mathrm{d}y'[\tilde{U}g_l^{(1)} + \overline{(U-\tilde{U})G^{(1)}}]\right)^2\right\}. \tag{10.3}$$

This enables us to rewrite (10.1b) and hence, the kurtosis (10.2b) in terms of $G^{(1)}(y)$.

Thus, the contribution from the main flow to the kurtosis can be defined as

$$K(\beta) = \frac{24tK^{(4)}(\beta)}{[2tD(\beta)]^2}, \tag{10.4a}$$

with

$$K^{(4)}(\beta) = \frac{1}{1+\beta}\frac{1}{a}\int_{-a}^{0} \mathrm{d}y$$
$$\times\frac{1}{\kappa}\left[\int_{-a}^{y} \mathrm{d}y'\left(\frac{(\bar{u}-u)(g+\beta f)}{(1+\beta)^2} + \frac{\overline{(u-\bar{u})(g+\beta f)}}{(1+\beta)^2} + \beta\frac{\bar{u}\bar{f}-u(g+\beta f)}{(1+\beta)^2}\right)\right]^2$$
$$-D(\beta)\frac{\overline{(g+\beta f)^2}+\beta\bar{f}^2}{(1+\beta)^3}. \tag{10.4b}$$

The negative values of (10.4b) are shown in figure 8 for constant κ with β for the three velocity profiles considered in Appendix A. However, for large β, the kurtosis $|K(\beta)|$ increases linearly with β.

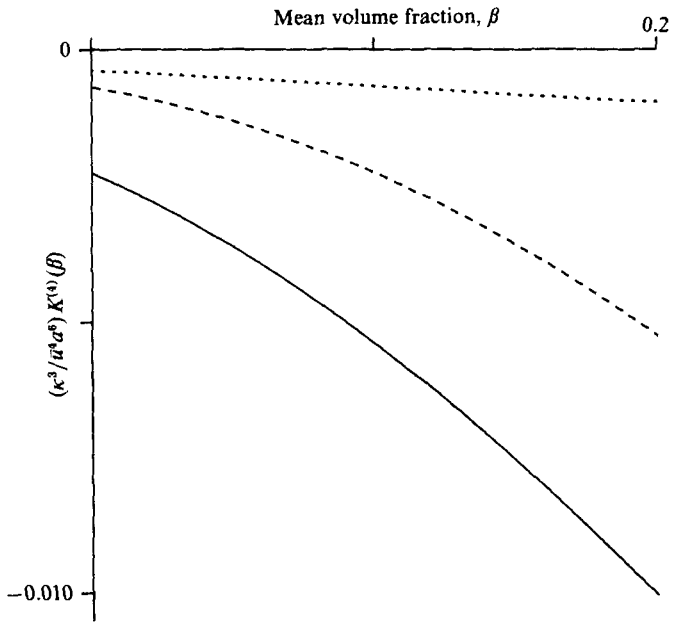

FIGURE 8. The values of $(\kappa^3/\bar{u}^4a^6)K^{(4)}(\beta)$ as a function of β for pipe Poiseuille flow (·····), plane Poiseuille flow (– – –) and Couette flow (——).

11. Mean concentration distribution

Although the widely used method of moments gives a great deal of information about the distributions of contaminant concentration across the flow as it disperses, nevertheless it has the disadvantage that it does not give a direct expression for C nor $\tilde{C}$. The details of the approach to normality of the mean concentration have been investigated by Chatwin (1970), who proposed an Edgeworth series expansion for $\tilde{C}$:

$$\tilde{C} = \frac{e^{-\frac{1}{2}X^2}}{(2\pi M^{(2)})^{\frac{1}{2}}}[1+\tfrac{1}{6}SH_3+\tfrac{1}{24}KH_4+\tfrac{1}{72}S^2H_6+O(t^{-\frac{3}{2}})], \tag{11.1}$$

with the longitudinal coordinate

$$X = \frac{x-\tilde{U}t}{(M^{(2)})^{\frac{1}{2}}}, \tag{11.2}$$

and H_3, H_4 and H_6 are Hermite polynomials defined by

$$H_3(X) = X^3-3X, \tag{11.3a}$$

$$H_4(X) = X^4-6X^2+3, \tag{11.3b}$$

$$H_6(X) = X^6-15X^4+45X^2-15. \tag{11.3c}$$

The complete Edgeworth series is infinite, and it involves all the cumulants, of which S and K are the first two. The series is believed to be asymptotic rather than convergent; unfortunately the sum of a finite number of terms of the series may give negative values (figure 9*a*), particularly near the tails where higher-order terms decrease in a somewhat irregular manner. This tendency is expected because, when the direct longitudinal diffusion is neglected, the concentration cannot be non-zero upstream of a point moving with the maximum velocity, nor downstream of a point

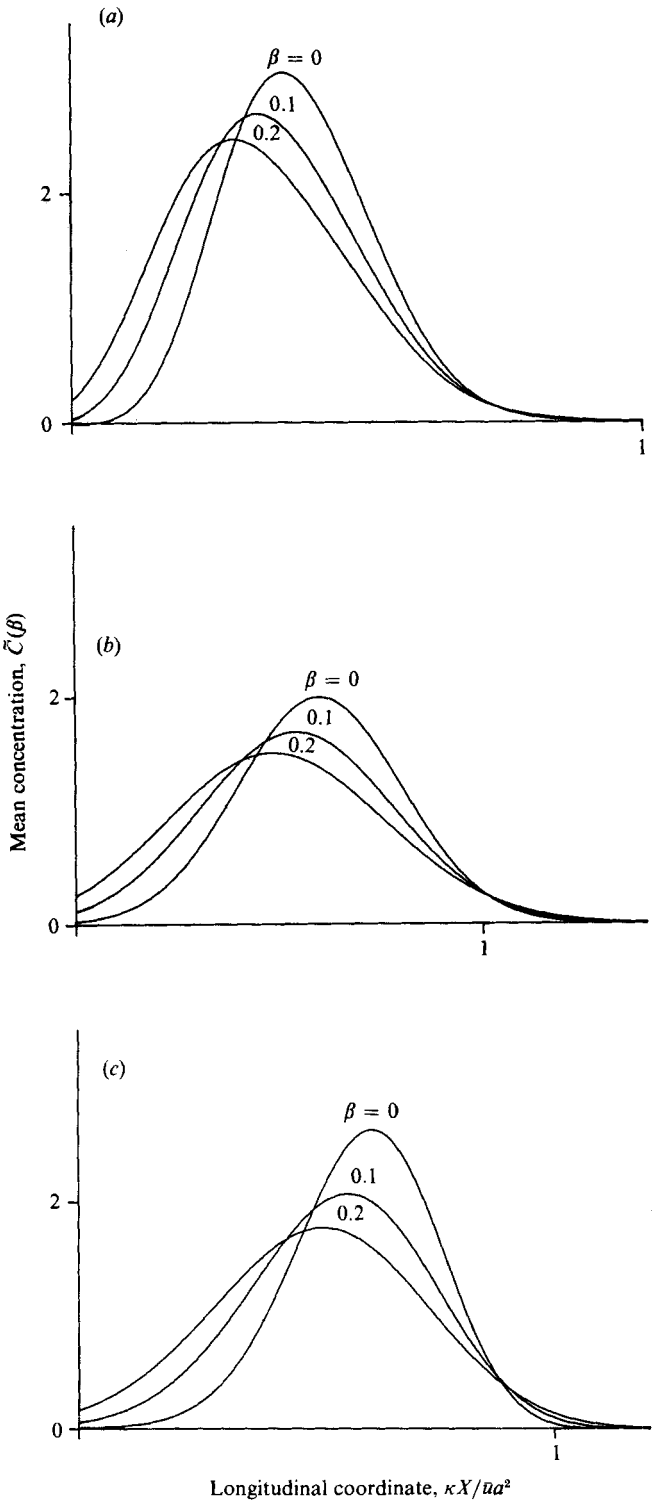

FIGURE 9. The Chatwin's (1970) Edgeworth series mean concentration $\tilde{C}(\beta)$ profiles as a function of $\kappa X/\bar{u}a^2$ at $6t_e(\beta = 0)$ after discharge. (*a*) Pipe Poiseuille flow; (*b*) Couette flow; (*c*) plane Poiseuille flow.

moving with the minimum velocity. Hence, $\tilde{C}$ must fall to zero more rapidly than the Gaussian profile. From (9.2) and (10.2*b*), the departure from the Gaussian profile is dominated, for large t, by the skewness. Smith (1982) conjectured that by neglecting K not only is (11.1) more accurate at large time, but also the combination of H_3 and H_6 ensures that the predicted concentrations are positive in the tails of contaminant distributions, except when the skewness is quite marked. For this reason, and for simplicity, figure 9(*a–c*) has been calculated this way.

The noteworthy features of figure 9(*a–c*) as β is increased are the lower concentration, the displaced (slow-moving) peaks and the extended tail.

12. Concluding remarks

We have generalized the work of Aris (1959) so that direct predictions for the first four moments of contaminant concentration distributions in the presence of dead zones are made in the manner advocated by Aris's (1956) conventional (no-pockets) method of moments. The mathematically preferred composite cross-sectional averaging process results are simpler in character as well as in mathematical form. The decompositions (4.7*a*, *b*) for the centroid displacement function $G^{(1)}(y)$ are straightforward to evaluate, and have been used to illuminate several facets of dispersion process. Furthermore, the decomposition (5.6) of the longitudinal dispersion coefficient reveals that the shear-dispersion coefficient D can be vastly increased by the introduction of dead zones. The asymptotic formulae (9.3) and (10.4*a*, *b*) demonstrate the individual role of the shear velocity, and the mean volume fraction β on the main-flow-related contribution to the skewness and to the kurtosis respectively.

The general conclusions obtained are believed to be applicable to real flows. Natural streams are subject to a long-term build-up of plant material, especially on the side boundary. This suggests that the flow field can be divided into main-flow and dead-zone regions, since the velocity fluctuations fall to zero and the intensity of lateral mixing decreases rapidly as the dead zones are approached. Here, dead zones may have circulating eddies; however so long as there is no net downstream advection within dead zones, we could treat them as stagnant pockets as far as the above analyses are concerned. The work of Young & Wallis (1986) suggests that values of β of the order of 0.15 are appropriate to real rivers. The results shown in figures 3 and 6 reveal the marked influence upon the spreading rate and the skewness when the dead-zones mean volume fraction has such large values.

I wish to thank my research supervisor, Dr R. Smith, who suggested the problem and provided continual advice, support and encouragement throughout the work. I should also like to thank the referees for their helpful comments. The financial support of an Overseas Research Student award is gratefully acknowledged.

Appendix A. Centroid displacement and other auxiliary functions

In the absence of stagnant pockets, the skewness is very sensitive to the main-flow velocity profiles. Firstly, we consider the dispersion of a passive contaminant with constant molecular diffusivities $\kappa_l = \kappa$ in the Couette flow. The linear main-flow velocity profile takes the form

$$u(Y) = 2\bar{u}\left(1-\frac{Y}{a}\right) \quad \text{for } 0 < Y < a, \tag{A 1}$$

where we have rescaled $Y = y+a$, and a is the channel depth.

To quantify the effect of the mean volume fraction β we need to calculate the auxiliary functions defined in (4.4a, b) and (4.8a–c)

$$g(Y) = \frac{\bar{u}a^2}{12\kappa}\left[1-6\left(\frac{Y}{a}\right)^2+4\left(\frac{Y}{a}\right)^3\right], \tag{A 2a}$$

$$f(Y) = \frac{\bar{u}a^2}{3\kappa}\left[\frac{\beta}{1+\beta}+1-3\left(\frac{Y}{a}\right)^2+\left(\frac{Y}{a}\right)^3\right], \tag{A 2b}$$

Next, from (8.7a, b), (8.12a–c) and (8.13a–c), we obtain

$$I(Y) = \frac{\bar{u}a^4}{120\kappa^2}\left[1-5\left(\frac{Y}{a}\right)^2+5\left(\frac{Y}{a}\right)^4-2\left(\frac{Y}{a}\right)^5\right], \tag{A 3a}$$

$$J_{(1)}(Y) = \frac{\bar{u}a^4}{60\kappa^2}\left[3-10\left(\frac{Y}{a}\right)^2+5\left(\frac{Y}{a}\right)^4-\left(\frac{Y}{a}\right)^5\right] + \frac{\bar{u}a^4}{180\kappa^2(1+\beta)}\beta\left[19-30\left(\frac{Y}{a}\right)^2+\frac{20\beta}{1+\beta}\right], \tag{A 3b}$$

$$J_{(2)}(Y) = \frac{a^2}{12\kappa}\left[3-6\left(\frac{Y}{a}\right)^2+\frac{8\beta}{1+\beta}\right]. \tag{A 3c}$$

It is now straightforward to evaluate all the necessary quantities for the contribution from the main-flow such as $D(\beta)$, $\lambda(\beta)$, $\widetilde{(U-\tilde{U})(G^{(1)})^2}(\beta)$ and $K^{(4)}(\beta)$.

The widely studied example of pipe Poiseuille flow is exceptional in that the dominant contribution to the skewness is anomalously small but positive. For laminar flow in a circular pipe of radius a, with constant molecular diffusivities $\kappa_l = \kappa$, the parabolic main-flow velocity profile is

$$u(r) = 2\bar{u}\left[1-\left(\frac{r}{a}\right)^2\right] \quad \text{for } 0 < r < a, \tag{A 4a}$$

where we have rescaled $r = y+a$. The circular symmetry means that we can restrict our attention to purely radial variation and, systematically, we are dealing with twice as much boundary per unit cross-sectional area. For example, the continuity of transverse flux boundary condition (3.2b) at the pipe wall $r = a$ becomes (Aris 1959)

$$2r\kappa\,\partial_r c = \{r\kappa_l\,\partial_y c_l\}, \tag{A 4b}$$

and subsequently, the factor *two* should be presented in any expression related to the cross-sectional area.

To quantify the effect of the mean volume fraction β we need to evaluate the auxiliary functions defined in (4.4a, b) and (4.8a–c):

$$g(r) = \frac{\bar{u}a^2}{24\kappa}\left[2-6\left(\frac{r}{a}\right)^2+3\left(\frac{r}{a}\right)^4\right], \tag{A 5a}$$

$$f(r) = \frac{\bar{u}a^2}{8\kappa}\left[\frac{\beta}{(1+\beta)}+2-4\left(\frac{r}{a}\right)^2+\left(\frac{r}{a}\right)^4\right]. \tag{A 5b}$$

Next, from (8.7*a*, *b*), (8.12*a*–*c*) and (8.13*a*–*c*), we derive

$$I(r) = \frac{\bar{u}a^4}{1152\kappa^2}\left[7-24\left(\frac{r}{a}\right)^2+18\left(\frac{r}{a}\right)^4-4\left(\frac{r}{a}\right)^6\right], \tag{A 6a}$$

$$J_{(1)}(r) = \frac{\bar{u}a^4}{288\kappa^2}\left[7-18\left(\frac{r}{a}\right)^2+9\left(\frac{r}{a}\right)^4-\left(\frac{r}{a}\right)^6\right]+\frac{\bar{u}a^4}{192\kappa^2(1+\beta)}\beta\left[5-6\left(\frac{r}{a}\right)^2+\frac{3\beta}{(1+\beta)}\right], \tag{A 6b}$$

$$J_{(2)}(r) = \frac{a^2}{12\kappa}\left[2-3\left(\frac{r}{a}\right)^2+\frac{3\beta}{(1+\beta)}\right]. \tag{A 6c}$$

These enable us to calculate all the necessary quantities contributed by the main-flow.

In the absence of stagnant pockets the contaminant concentration distribution in plane Poiseuille flow with constant molcular diffusivities $\kappa_l = \kappa$ has a negative skewness (Jayaraj & Subramanian 1978). The main-flow velocity profile takes the form

$$u(Y) = \tfrac{3}{2}\bar{u}\left[1-\left(\frac{Y}{a}\right)^2\right] \quad \text{for } 0 < Y < a, \tag{A 7}$$

where we have rescaled $Y = y+a$, and $2a$ is the separation channel width.

To quantify the effect of the mean volume fraction β we need to determine the auxiliary functions defined in (4.4*a*, *b*) and (4.8*a*–*c*):

$$g(Y) = \frac{\bar{u}a^2}{120\kappa}\left[7-30\left(\frac{Y}{a}\right)^2+15\left(\frac{Y}{a}\right)^4\right], \tag{A 8a}$$

$$f(Y) = \frac{\bar{u}a^2}{24\kappa}\left[\frac{8\beta}{1+\beta}+7-18\left(\frac{Y}{a}\right)^2+3\left(\frac{Y}{a}\right)^4\right]. \tag{A 8b}$$

Next, from (8.7*a*, *b*), (8.12*a*–*c*) and (8.13*a*–*c*), we derive

$$I(Y) = \frac{\bar{u}a^4}{5040\kappa^2}\left[31-147\left(\frac{Y}{a}\right)^2+105\left(\frac{Y}{a}\right)^4-21\left(\frac{Y}{a}\right)^6\right], \tag{A 9a}$$

$$J_{(1)}(Y) = \frac{\bar{u}a^4}{720\kappa^2}\left[31-105\left(\frac{Y}{a}\right)^2+45\left(\frac{Y}{a}\right)^4-3\left(\frac{Y}{a}\right)^6\right] + \frac{\bar{u}a^4}{90\kappa^2(1+\beta)}\beta\left[9-15\left(\frac{Y}{a}\right)^2+\frac{10\beta}{(1+\beta)}\right], \tag{A 9b}$$

$$J_{(2)}(Y) = \frac{a^2}{30\kappa}\left[7-15\left(\frac{Y}{a}\right)^2+\frac{20\beta}{1+\beta}\right]. \tag{A 9c}$$

Again from (A 8*a*, *b*) and (A 9*a*–*c*), we can determine all the necessary quantities contributed by the main flow.

Appendix B. The one-sided Gaussian stagnant-pocket depths

Naturally, the mean volume fraction β has a more direct physical interpretation than any other stagnant-pockets property, but there is also more complex dependence on the statistics of $p(l)$ as was first pointed out by Aris (1959). For

illustration, we consider a simple case for which the pocket depths are distributed according to the one-sided Gaussian with the mean volume fraction β as its parameter. Then

$$p(l) = \frac{2}{\pi\beta} e^{-l^2/\pi\beta^2}, \quad \{l^{2n}\} = \frac{1.3.5....(2n-1)}{2}(\pi\beta^2)^n,$$

$$\{l^{2n+1}\} = \beta n!(\pi\beta^2)^n \quad n = 1, 2, 3, ...$$

The factorial stems from the sensitivity of the higher moments to the occasional deep pocket.

The stagnant-pocket property term E can increase the value of $D(\beta)$ as much as 15% for the pipe Poiseuille flow with $\beta = 0.2$. Similarly, $p(l)$ alone contributes 24% to $\widetilde{(G^{(1)})^2}(\beta)$, whereas the stagnant-pocket property term H contributes a further 18%. Thus, the additional decreasing of the decay rate $\lambda(\beta)$ due to the pocket-depths statistics cross-term (6.3a) amounts to more than 19% for the one-sided Gaussian stagnant-pocket depths with $\beta = 0.2$.

Although the stagnant-pocket property term L contribution is always negative, as is the $p(l)$-related contribution for the pipe Poiseuille flow, provided $\beta \leqslant 0.41$, for $\beta = 0.2$ the combination of these terms is still not enough to exceed the positive main-flow-related contribution $\widetilde{(U-\tilde{U})(G^{(1)})^2}(\beta)$. The L-term reduces its value by 42%, and the one-sided Gaussian stagnant-pocket depths term reduces it further by 16%.

REFERENCES

Aris, R. 1956 On the dispersion of a solute in a fluid flowing through a tube. *Proc. R. Soc. Lond.* A**235**, 67–77.

Aris, R. 1959 The longitudinal diffusion coefficient in flow through a tube with stagnant pockets. *Chem. Engng Sci.* **11**, 194–198.

Barton, N. G. 1983 On the method of moments for solute dispersion. *J. Fluid Mech.* **126**, 205–218.

Chatwin, P. C. 1970 The approach to normality of the concentration distribution of a solute in a solvent flowing along a straight pipe. *J. Fluid Mech.* **43**, 321–352.

Chatwin, P. C. 1973 A calculation illustrating effects of the viscous sub-layer on longitudinal dispersion. *Q. J. Mech. Appl. Maths* **26**, 427–439.

Chatwin, P. C. 1980 Presentation of longitudinal dispersion data. *Proc. ASCE, J. Hydraul. Div.* **106**, 71–83.

Evans, E. V. & Kenney, C. N. 1966 Gaseous dispersion in laminar flow through a circular tube with mass transfer to a retentive layer. *Proc. R. Soc. Lond.* A**293**, 562–572.

Fischer, H. B. 1967 The mechanics of dispersion in natural streams. *Proc. ASCE, J. Hydraul. Div.* **93**, 187–216.

Jayaraj, K. & Subramanian, R. S. 1978 On relaxation phenomena in field-flow fractionation. *Sep. Sci. Tech.* **13**, 791–817.

Nordin, C. F. & Troutman, B. M. 1980 Longitudinal dispersion in rivers: the persistence of skewness in observed data. *Wat. Resour. Res.* **16**, 123–128.

Okubo, A. 1973 Effect of shoreline irregularities on streamwise dispersion in estuaries and other embayments. *Neth. J. Sea Resp.* **6**, 213–224.

Smith, R. 1981*a* A delay-diffusion description for contaminant dispersion. *J. Fluid Mech.* **105**, 469–486.

Smith, R. 1981*b* The importance of discharge siting upon contaminant dispersion in narrow rivers and estuaries. *J. Fluid Mech.* **108**, 43–53.

Smith, R. 1982 Gaussian approximation for contaminant dispersion. *Q. J. Mech. Appl. Maths* **35**, 345–366.

SMITH, R. 1985 When and where to put discharge in an oscillatory flow. *J. Fluid Mech.* **153**, 479–499.

TAYLOR, G. I. 1953 Dispersion of soluble matter in solvent flowing slowly through a tube. *Proc. R. Soc. Lond.* A**219**, 186–203.

TURNER, G. A. 1958 The flow-structure in packed beds. *Chem. Engng Sci.* **7**, 156–165.

VALENTINE, E. M. & WOOD, I. R. 1977 Longitudinal dispersion with dead zones. *Proc. ASCE, J. Hydraul. Div.* **103**, 975–990.

YOUNG, P. C. & WALLIS, S. G. 1986 The aggregated dead zone (ADZ) model for dispersion in rivers. *Intl Conf. on Water Quality Modelling in the Inland Natural Environment, Bournemouth, England*, pp. 421–433. BHRA.